Fast-Response Pyrometer Development for Expansion Tunnel Testing with Hot Carbon Models

E. J. Fahy[1], **F. Zander**[1], **D. R. Buttsworth**[2] **and R. G. Morgan**[1]

[1]Centre for Hypersonics
University of Queensland, Queensland 4072, Australia

[2]Computational Engineering and Science Research Centre
University of Southern Queensland, Toowoomba, Queensland 4350, Australia

Abstract

New methods for hot wall testing in expansion tunnels allow more accurate simulation of re-entry flow characteristics through resistive heating of carbon-carbon models to above 2000 K, representative of levels reached in flight. A non-intrusive, fast-response spectral pyrometer has been developed to measure surface temperature variations during the short steady flow time in expansion tunnel tests, and deduce surface heat flux through an unsteady heat conduction model. The signal is converted to spectral irradiance, and for gray bodies, the ratio between the irradiance of any two of four filter wavelengths allows deduction of surface temperature. To use the system for time accurate measurements through the radiating shock layer of re-entry bodies, non-emitting windows in the spectrum have been identified. The pyrometer has been spectrally calibrated using a tungsten lamp and its performance independently checked through benchtop testing of carbon-carbon samples at measured temperatures. The capacity to measure temperature and heat flux on carbon-carbon models at elevated surface temperatures, combined with emission spectroscopy of the shock layer will provide the opportunity to explore previously inaccessible flow thermochemistry interactions with heat shield materials under realistic re-entry conditions.

Introduction

The Hayabusa asteroid sample return mission landed at Woomera in 2010, providing a unique opportunity to gather re-entry data for comparison with ground testing in hypersonic impulse facilities, such as the University of Queensland's expansion tunnel facility. The X2 expansion tunnel is used to test subscale models at flight equivalent flow conditions, and a range of spectrometry and imaging techniques observe and record features of the flow. Conditions can be developed to simulate points of interest of the Hayabusa re-entry trajectory. Flight equivalent speeds of up to 10 km/s can can be simulated with test times in the order of $100 - 150$ μs. A new procedure developed by Zander et al [1] to heat carbon-carbon models to temperatures above 2000 K allows more realistic conditions to be achieved than with traditional cold wall tests. The maximum temperature experienced by Hayabusa's thermal shields was approximately 2500 K [2], hence a subscale heated carbon model, which is heated to the flight temperature, is proposed for testing in X2. To measure the surface temperature of the carbon-carbon model and its variation over the steady test time, a pyrometer has been developed and calibrated. Pyrometers are non-intrusive, so the flow is not disrupted, have fast response times, crucial for a facility with such short test times, and the ability to measure the change in surface temperature during the entire test time [3]. In order to observe as much of the test time as possible, a frequency resolution of 1 MHz for the detectors is required. The pyrometer has been calibrated for temperature response, its time response was verified, and initial benchtop tests were conducted with hot carbon models to prepare for tunnel testing. A digital single-lens-reflex (DSLR) camera image,

Figure 1: Pyrometer front, showing 2×2 arrangement of lenses. Filters and detectors are connected behind lenses.

which has been post-processed using a two colour ratio method, has been provided for comparison with results from the pyrometer, as this method has been previously tested on heated carbon models [1].

Pyrometer Setup

The pyrometer is comprised of four plano-convex lenses, four filters and four detectors mounted in a 2×2 arrangement, as shown in Figure 1. Light from a source passes through the convex side of the lens, through the filter and is focused onto the detector (Figure 2). There are two detectors that are most sensitive in the visible wavelengths and two in the infrared, and four narrow wavelength band filters that are centred at 450 nm, 700 nm, 1100 nm and 1600 nm. These centre wavelengths were selected because there are no strong emission lines in the wavelength bands around each centre, demonstrated by Hayabusa flight data from Buttsworth et al [4] and McIntyre et al [5], spectral data from a subscale Hayabusa model [4] and computational fluid dynamics (CFD) of Hayabusa flowfields [**?**]. Data cables run from the detector to an oscilloscope or data acquisition system, and a terminating resistor matched to each detector enables a sufficiently fast time response. The output signal from the detectors is a voltage and pairs of voltages can be converted to a spectral irradiance ratio through Equation 1.

$$\frac{I_2}{I_1} = \frac{V_2}{V_1} \frac{R_1 A W_1 A_{s1} \Omega_1 \lambda_{band,1}}{R_2 A W_2 A_{s2} \Omega_2 \lambda_{band,2}} \qquad (1)$$

Factors used in the conversion include the terminating resistance R, an amps per watt factor AW provided by the manufacturer for each detector, the wavelength band of the narrow pass filter, the source area A_s and the solid angle Ω.

From the ratio of irradiance for pairs of detectors, it is possible to deduce the temperature from the Planck curve under the assumption of a gray body. An alternative approach is to perform a non-linear least squares error fit to results from all four detectors. Results from both approaches are presented in this paper.
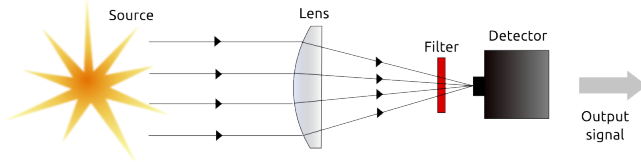
Figure 2: The configuration of one pyrometer channel. The pyrometer consists of four channels that operate in this fashion.

Calibration and Verification

To capture the temperature of the heated model in the extremely short test times of the X2 expansion tunnel, the pyrometer needs to be spectrally calibrated using a two colour ratio method, and its time response needs to be verified. These objectives were achieved using a tungsten calibration lamp of known irradiance and a white light emitting diode (LED) switching on.

Spectral Calibration

The pyrometer was calibrated with a tungsten filament lamp which has known spectral irradiance at a distance of 500 mm. The lamp was located centrally to the four lenses at distances of 500 mm, to compare to known values, and 600 mm, the distance at which the pyrometer will sit from the centreline of the model in the X2 expansion tunnel.

Each detector-lens system was moved using coarse and fine adjustments until the voltage output reading was maximised. As there was no method to quantitatively move and position the detector-lens systems, careful alignment was required to find the position for maximum voltage, although several attempts at alignment proved it is repeatable by measuring the same maximum output voltage.

Voltage measurements were taken with two sets of resistors: the first (referred to as 'normal' resistors) are required for the fast response times necessary in expansion tunnel use but give small voltage readings, and the second set are all 1 MΩ resistors, for which time response is sacrificed for higher voltage readings. Resistances of the 'normal' resistors were 8 kΩ and 1 kΩ for the 450 nm and 700 nm detectors, and 500 Ω for the 1100 nm and 1600 nm detectors. Use of the resistors is further discussed in the 'Benchtop Testing with Hot Carbon Models' section.

Sensitivity values for each detector, S_{det}, were calculated for each channel in units of $(W/m^2 \; nm)/V$, demonstrating the sensitivity of spectral irradiance to a change in measured voltage. Equation 2 calculates the irradiance, I, in benchtop tests from the measured voltage with background removed and the sensitivity.

$$I = \frac{V - V_{background}}{S_{det}} \qquad (2)$$

The irradiance ratio of each wavelength pair was compared to the corresponding irradiance ratio calculated using the known irradiance data for the lamp, and a calibration factor was determined from the relative difference of the measured and theoretical irradiance ratio for each wavelength pair. The calibration factors include differences between actual and theoretical ratios caused by distance and resistance changes, as well as losses caused by the optics or electrical system. These factors were used to calculate the irradiance ratio from the output voltage and find the resulting temperature. The effective temperature of the calibration lamp was measured for each ratio, and values range from 3116 K to 3185 K.

Time Response Verification

Time response verification of the pyrometer is important because the response times need to be much less than the X2 expansion tunnel steady test time of approximately 100 μs. The response of each detector was tested by switching on a bright, white light LED positioned directly in front of each detector, without the lens or filter attached. The data was recorded on a digital oscilloscope with an external trigger setting. The fastest time response was from detector 1, which is most sensitive in the infrared, and the slowest time response was from detector 4, most sensitive in the visible spectrum. Figure 3 shows the raw response from detector 1 in blue, and from detector 4 in red. The difference in magnitude of voltage readings occurs because the visible detectors are much more sensitive to the LED than the infrared detectors, and the terminating resistors on the visible detectors differ. Figure 3 shows that the response time of each detector, between 10 % and 90 % of the peak value, is approximately 2 μs, demonstrating that the detectors with the selected resistors have a sufficiently fast response to observe changes within the steady test time.
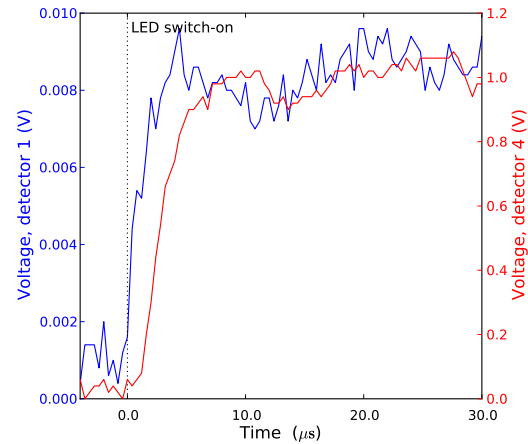
Figure 3: Time response of detectors 1(700-1800 nm) and 4 (200-1100 nm) using switch-on of a white light LED.

A Savitzky-Golay filter can also be applied to remove high-frequency noise through a low-pass filter and least-squares polynomial fitting in a post-processing code [7]. The magnitude of noise in tunnel test data will influence how easily the signal from a change in temperature will be resolved. In Figure 3, the maximum noise in the detector 1 and 4 signals is 20 % and 5 % of the maximum voltage, respectively.

Benchtop Testing with Hot Carbon Models

Benchtop testing of the pyrometer looking at a heated carbon model was used to test the spectral calibration and investigate whether the calculated temperatures from non-linear Planck curve fitting, and two colour ratio pyrometry with a DSLR image or between pairs of filter wavelengths, are comparable.

The carbon fibre test pieces were hemi-cylindrical, with a radius

of 28 mm, width of 10 mm, and thickness of 3 mm. Tests were conducted in air at atmospheric pressure, and the laboratory was well-vented to remove fumes from ablation of the matrix. The input voltage and current were approximately 10 V and 200 A once the resistance in the carbon model dropped due to heating, providing a power through the model of approximately 2 kW. The first test was performed with the 'normal' resistors required for the short response times necessary in the tunnel, resulting in small values for measured voltages, especially for the 450 nm filter. To increase the voltage output, a second test was performed with 1 MΩ resistors on each detector as temperature and not time response was the desired result of these benchtop tests. The background noise was recorded and removed from the signals for both tests, and samples were taken over 10 seconds once the model had reached thermal equilibrium. Voltage measurements were converted to spectral irradiance using Equation 2 and the calibration factor determined from the lamp data was applied.
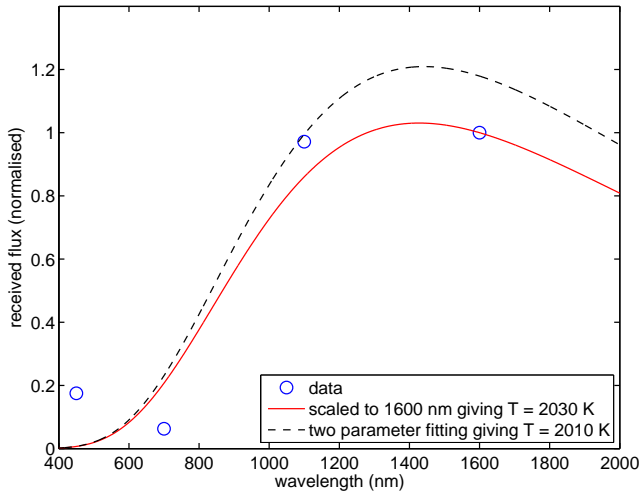
Figure 4: Measured hot carbon spectral irradiance for four wavelengths, normalised using the 1600 nm result.

Non-linear Planck curve fitting was employed to the measured hot carbon spectral irradiance for four wavelengths to determine the temperature, and the results shown in Figure 4 were normalised using the 1600 nm result. Two different Planck curve results are shown. In the case of the solid line, a Planck curve which matches the irradiance at 1600 nm has been identified by minimising the least-squares error for the 450, 700, and 1100 nm irradiance values, yielding a temperature of 2030 K. In the case of the broken line, the least-squares error minimisation strategy is applied to all four wavelength results through the use of two fitting parameters: the temperature, and a magnitude scaling parameter. The temperature deduced in this case was 2010 K.

A DSLR image was taken during test 2 and postprocessed using the two colour ratio pyrometry methods described in Zander et al [1]. The images for the various colour ratios produced from the original DSLR image are shown in Figure 5, and the calculated average temperature is approximately 2050 K. This compares well to the deduced temperatures of 2010 K and 2030 K using the Planck curve fitting described above.

Figure 6 shows the temperature calculated from each wavelength ratio for test 2, and selected ratios from test 1, with error bars. These results were calculated using a two colour ratio method for the ratios of two wavelengths, where the lamp calibration factor is scaled by the temperature of the lamp relative

to the heated carbon model. Ratios involving the 450 nm detector in test 1 have been neglected from these results because the voltage measurement was similar to the background noise. The 450 nm detector will still be tested on the expansion tunnel to determine whether a signal is resolvable above noise. The average temperature from these results was 2067 K.
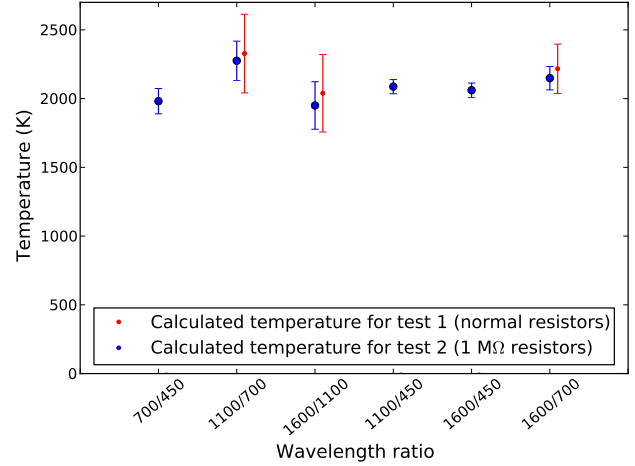
Figure 6: Temperature calculated from each wavelength ratio for test 1 (normal resistors) and test 2 (1 MΩ resistors) using a hot carbon model.

$$s_f = \sqrt{\left(\frac{\partial f}{\partial x_1}\right)^2 s_{x_1}^2 + \left(\frac{\partial f}{\partial x_2}\right)^2 s_{x_2}^2 + \left(\frac{\partial f}{\partial x_3}\right)^2 s_{x_3}^2 + ...} \quad (3)$$

The error bars were determined using Equation 3 to calculate error propagation for independent variables. The total error, s_f, in the temperature f is calculated through the change in f for the change in each variable, and the error in each variable. The variables that can cause error in calculation of temperature are the voltage, the effective observation area of the detector to the model, the solid angle, caused by the distance between the system and the source, and an error in the centre wavelength. Values of the derivative term and the error in the variable were tabulated for each ratio in both tests, and the resulting value of s_f produced the error bars for Figure 6. The average irradiance over a filter wavelength band gave the same result as the central wavelength irradiance when using values from a Planck curve, hence an error over the band was neglected. A gray body assumption dictates that emissivity has no wavelength dependence and can therefore be neglected from the analysis.

This method is still under development and although results compare well with the results from the benchtop tests and the calibration lamp data, further verification and refinement is needed and will continue with upcoming tests involving the pyrometer.

Application

The pyrometer has been developed to observe heated carbon models in the X2 expansion tunnel, and observe the temperature of the model throughout the steady test time. It is important to determine whether expected temperature changes will be resolvable based on results from calibration and benchtop testing.

The following properties have been assumed for a carbon composite model: density, $\rho = 1300$ kg/m^3, specific heat, $c_p =$
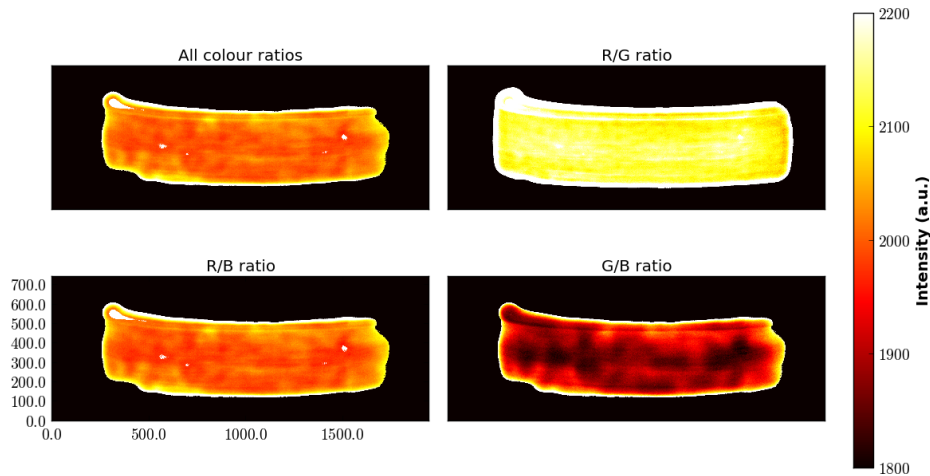
Figure 5: Temperature calculated from DSLR image for test 2 using a hot carbon model.

700 J/kg K and thermal conductivity, $k = 1.0$ W/m K. Assuming a stagnation point heat flux $\dot{q} = 15$ MW/m^2 and a steady test time $dt = 100$ μs, the expected change in temperature is approximately 170 K using Equation 4.

$$dT = \frac{2q_s\sqrt{t}}{\sqrt{\pi\rho c_p k}} \qquad (4)$$

A temperature rise of this magnitude would cause an increase in voltage on the order of several mV, which should be detectable for the 700 nm, 1100 nm and 1600 nm detectors based on the voltage measured in benchtop testing and noise measured in time response testing. The signal from the 450 nm detector could be problematic if the source is not bright enough to produce a signal that is greater than the noise level. However, if initial tests prove that the 450 nm detector signal is not resolvable, there are still three useable ratios from other detectors, or it can be substituted for a higher wavelength detector.

Conclusion

The development of a fast response pyrometer for measuring surface temperatures of heated models (in expansion tunnels) has been presented. The pyrometer was calibrated using a tungsten lamp for temperature, verified for time response using a white light LED, and benchtop testing was conducted with a heated carbon model. Initial calibration and testing indicates that the pyrometer has been developed to be capable of 1MHz measurements and sensitive enough to detect the expected change in surface temperature during the short test time. Future work includes the testing of a heated model in the X2 expansion tunnel to investigate the surface temperature and its variation during a test at flight equivalent flow conditions.

Acknowledgements

References

[1] Zander, F., Morgan, R.G., Sheikh, U.A., Buttsworth, D.R. and Teakle, P.R., Hot Wall Re-Entry Testing in Hypersonic Impulse Facilities, *AIAA Journal* (accepted subject to editorial corrections), 2012.

[2] Abe, S., Fujita, K., Kakinami, Y., Iiyama, O., Kuroaki, H., Shoemaker, M.A., Shiba, Y., Ueda, M. and Suzuki, M., Near-Ultraviolet and Visible Spectroscopy of Hayabusa Spacecraft Re-Entry, *Publications of the Astronomical Society of Japan*, 63(5), pp 1011-1021, 2011.

[3] Gulhan, A., Application of Pyrometry and IR-Thermography to High Surface Temperature Measurements, *RTO AVT Course on 'Measurement Techniques for High Enthalpy and Plasma Flows'*, Belgium, October 25-29, 1999.

[4] Buttsworth, D.R., Jacobs, P., Potter, D., Mudford, N., D'Souza, M., Eichmann, T., Jenniskens, P., McIntyre, T., Jokic, M., Jacobs, C., Upcroft, B., Khan, R., Porat, H., Neely, A. and Lohle, S., Super-Orbital Re-Entry in Australia: Laboratory Measurement, Simulation and Flight Observation, *28th International Symposium on Shock Waves*, Manchester, UK, 2011.

[5] McIntyre, T., Khan, R., Eichmann, T., and Upcroft, B., Visible and Near Infrared Spectroscopy of Hayabusa Re-Entry using Semi-Autonomous Tracking, *50th AIAA Aerospace Sciences Meeting*, Nashville, USA, 2012.

[6] Potter, D., Modelling of Radiating Shock Layers for Atmospheric Entry at Earth and Mars, Ph.D. Dissertation, Centre for Hypersonics, University of Queensland, Australia, 2011.

[7] Savitzky, A., and Golay, M. J. E., Smoothing and Differentiation of Data by Simplified Least Squares Procedures. *Analytical Chemistry*, 1964, 36 (8), pp 1627-1639.